PHENIX measurements of 3D emission source functions in Au+Au collisions at $\sqrt{s_{NN}} = 200$ GeV

Roy A. Lacey for the PHENIX Collaboration

Department of Chemisry, Stony Brook University, Stony Brook, NY 11794-3400, USA

E-mail: Roy.Lacey@Stonybrook.edu

Abstract. A state-of-the-art 3D source imaging technique is used to extract the 3D two-pion source function in central and mid-central Au+Au collisions at $\sqrt{s_{NN}} = 200$ GeV. The source function indicates a previously unresolved non-Gaussian tail in the directions of the pion pair transverse momentum (out) and along the beam (long). Model comparisons give robust estimates for several characteristics of the emission source, including its transverse size, its mean proper breakup time τ and its emission duration $\Delta\tau$. These estimates are incompatible with the predictions for a first order phase transition. However, they point to significant relative emission times which could result from a crossover phase transition.

1. Introduction

Lattice calculations indicate a rapid transition from a confined hadronic phase to a chirally symmetric de-confined quark gluon plasma (QGP) at the critical temperature $T_c \sim 170$ MeV [1]. Such a plasma is produced in energetic Au+Au collisions at the Relativistic Heavy Ion Collider RHIC. However, it is currently unclear whether the phase transition to the QGP phase is first order ($\Delta T = 0$) or a rapid crossover reflecting an increase in the entropy density associated with the change from hadronic (d_H) to quark and gluon (d_Q) degrees of freedom.

An emitting system which undergoes a first order phase transition is predicted to have a large space-time extent [2, 3]. This is because the transition "softens" the equation of state (ie. the sound speed $c_s \sim 0$) in the transition region, and this delays the expansion and considerably prolongs the lifetime of the system. A smaller space-time extent has been predicted for systems which undergo a crossover transition [3].

To search for a prolonged lifetime, it has been a common practice to measure the widths (R) of the emission source function (assumed to be Gaussian) in the out- side- and long-direction (R_{out}, R_{side} and R_{long}) of the Bertsch-Pratt coordinate system [4]. Here, the prediction is that $R_{out}/R_{side} >> 1$, for systems which undergo a first order phase transition, [2, 3]. This is illustrated in Fig. 1, where the values obtained from a hydrodynamical model calculation [3] are plotted as a function of energy density (in units of $T_c s_c$; s is the entropy density).

These rather large ratios (cf. Figs. 1a and c) have served as a major motivating factor for experimental searches at several accelerator facilities [4]. No evidence for a prolonged lifetime were found by these studies and the reported Gaussian source functions are spheroidal with $R_{out} \approx R_{side}$ in the longitudinally co-moving system.

A crossover transition can be modeled by varying the width ΔT, of the transition region. Figs. 1a and b show that the magnitude of R_{out}/R_{side} is considerably reduced (by as much as a factor of four) when calculations are performed for $\Delta T = 0.1T_c$. Thus, the space-time extent of the emitting system is significantly influenced by the cross over transition and this could lead to less prominent signals which require more sensitive methods of detection. Indeed, a recent study with a 1D source imaging technique has observed a long non-Gaussian tail in the radial source function and attributed it to possible lifetime effects [5].
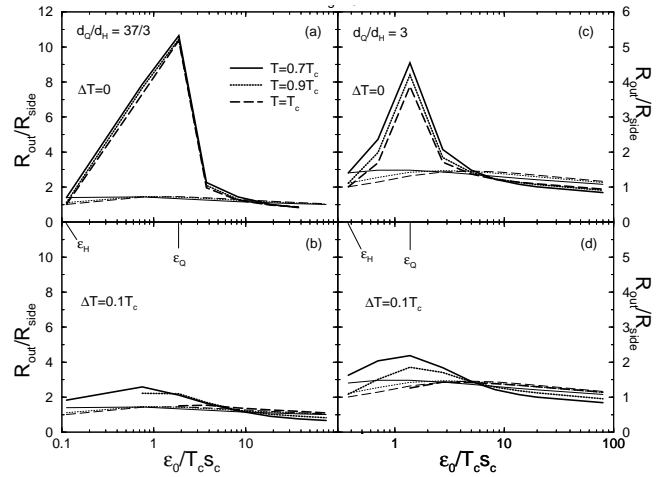

Figure 1: R_{out}/R_{side} as a function of the initial energy density for an expanding fireball. (a,b) are for $d_Q/d_H = 37/3$, (c,d) for $d_Q/d_H = 3$. The thick lines in (a,c) are for $\Delta T = 0$, in (b,d) for $\Delta T = 0.1T_c$. Thin lines show results for an ideal gas case. Solid lines show results for $T = 0.7T_c$, dotted for $T = 0.9T_c$, dashed for $T = T_c$. The figure is taken from Ref. [3].

In this contribution, we report on recent efforts to study the 3D two-pion source function via a new state-of-the-art technique proposed by Danielewicz and Pratt [6]. Namely, the 3D correlation function is first decomposed into a basis of Cartesian surface-spherical harmonics to extract the coefficients, also called moments, of the expansion. They are then imaged or fitted with a trial function to extract the 3D source function, which is then used to probe the emission dynamics of the pion source [7, 8].

2. Analysis Method

The 3D correlation function $C(\mathbf{q}) = N_{\text{fgd}}(\mathbf{q})/N_{\text{bkg}}(\mathbf{q})$ was obtained by taking the ratio of the 3D relative momentum distribution for $\pi^+\pi^+$ and $\pi^-\pi^-$ pairs in the same event $N_{\text{fgd}}(\mathbf{q})$ and those from mixed events $N_{\text{bkg}}(\mathbf{q})$, where $\mathbf{q} = \frac{(\mathbf{p_1}-\mathbf{p_2})}{2}$ where $\mathbf{p_1}$ and $\mathbf{p_2}$ are the momentum 4-vectors in the pair center of mass system (PCMS).

The 3D correlation function $C(\mathbf{q})$ was expanded in a Cartesian harmonic basis [6] to obtain the moments

$$C(\mathbf{q}) - 1 = R(\mathbf{q}) = \sum_{l,\alpha_1...\alpha_l} R^l_{\alpha_1...\alpha_l}(q)\, A^l_{\alpha_1...\alpha_l}(\Omega_\mathbf{q}) \tag{1}$$

where $l = 0, 1, 2, \ldots$, $\alpha_i = x, y$ or z, $A^l_{\alpha_1...\alpha_l}(\Omega_\mathbf{q})$ are Cartesian harmonic basis elements; ($\Omega_\mathbf{q}$ is the solid angle in $\mathbf{q}$ space); $R^l_{\alpha_1...\alpha_l}(q)$ are Cartesian correlation moments given

by Eq. (2); and q is the modulus of $\mathbf{q}$.

$$R^l_{\alpha_1...\alpha_l}(q) = \frac{(2l+1)!!}{l!} \int \frac{d\Omega_\mathbf{q}}{4\pi} A^l_{\alpha_1...\alpha_l}(\Omega_\mathbf{q})\, R(\mathbf{q}). \qquad (2)$$

Here, the coordinate axes are oriented so that z (long) is parallel to the beam direction and x (out) points in the direction of the total transverse momentum of the pair. For this analysis, Eq. (1) was truncated at $l = 6$ and expressed in terms of its 10 independent even moments: R^0, R^2_{x2}, R^2_{y2}, R^4_{x4}, R^4_{y4}, R^4_{x2y2}, R^6_{x6}, R^6_{y6}, R^6_{x4y2} and R^6_{x2y4} (R^2_{x2} is shorthand for R^2_{xx} [6]); odd moments were checked and found to be consistent with zero [within statistical uncertainty] as required by symmetry considerations; higher order moments (for $l > 6$) were also checked and found to be negligible.

The independent moments are shown as a function of q in Fig. 2. They were obtained by fitting the truncated series to the measured 3D correlation function with the moments as the parameters of the fit. It is noteworthy that the very good agreement between $R^0(q)$ and $R(q)$ (shown in panel (a)) points to the absence of any significant angular acceptance issues. It also attests to the reliability of the moment extraction technique. $R^0(q)$ and $R(q)$ both represent angle-averaged correlation functions, but $R^0(q)$ is obtained from the 3D correlation function via Eq. (2) while $R(q)$ is evaluated directly from the 1D correlation function as in Ref. [5].
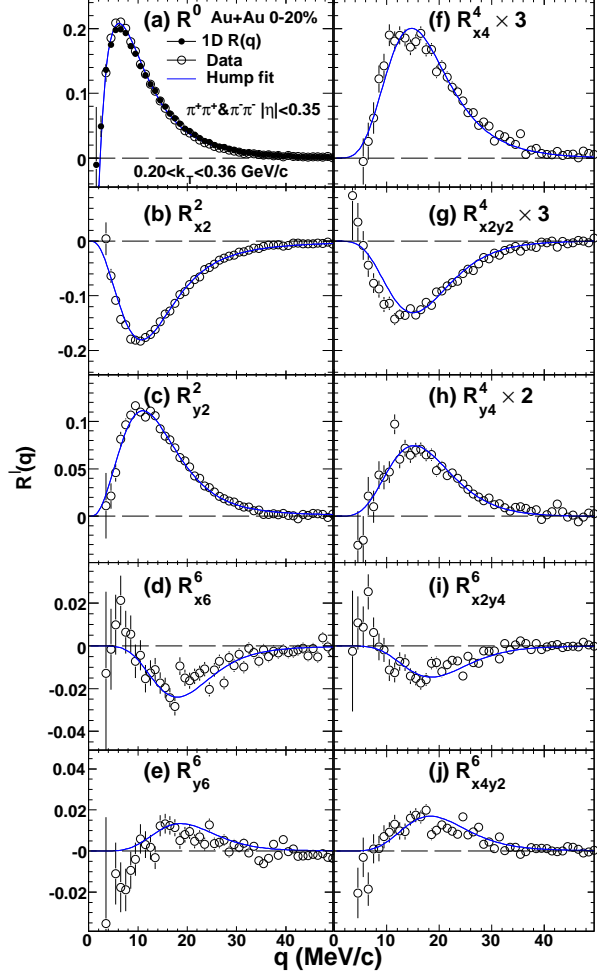

Figure 2: Experimental correlation moments $R^l(q)$ for l = 0, 2, 4, 6. Panel (a) also shows a comparison between $R^0(q)$ and $R(q)$. Systematic errors are less than the statistical errors. The solid curves indicate the Hump function Eq. (6) fit.

The 3D source function $S(\mathbf{r})$ is obtained from the moments via imaging or fitting. This is made transparent by the observation that, in analogy to Eq. (1), $S(\mathbf{r})$ can also be expanded in a Cartesian Surface-spherical harmonic basis

$$S(\mathbf{r}) = \sum_l \sum_{\alpha_1...\alpha_l} S^l_{\alpha_1...\alpha_l}(r)\, A^l_{\alpha_1...\alpha_l}(\Omega_\mathbf{r}). \qquad (3)$$

If the series for $R(\mathbf{q})$ and $S(\mathbf{r})$ are now substituted into the 3D Koonin-Pratt equation;

$$C(\mathbf{q}) - 1 = R(\mathbf{q}) = \int d\mathbf{r}\, K(\mathbf{q}, \mathbf{r}) S(\mathbf{r}), \qquad (4)$$

then, the following set of 1D expressions (Eq. (5)) [6] which relate the correlation moments $R^l_{\alpha_1...\alpha_l}(q)$ to the source moments $S^l_{\alpha_1...\alpha_l}(r)$ are obtained;

$$R^l_{\alpha_1...\alpha_l}(q) = 4\pi \int dr r^2 K_l(q,r) S^l_{\alpha_1...\alpha_l}(r). \tag{5}$$

Here, it should be noted that $S(\mathbf{r})$ gives the probability of emitting a pair of particles with a separation vector $\mathbf{r}$ in the PCMS and the 3D Kernel, $K(\mathbf{q},\mathbf{r})$, incorporates both the Coulomb force and the Bose-Einstein symmetrization.

The 1D imaging code of Brown and Danielewicz [9] was used to numerically invert each correlation moment $R^l_{\alpha_1...\alpha_l}(q)$ to extract the corresponding source moment $S^l_{\alpha_1...\alpha_l}(r)$. The latter were then combined as in Eq. (3), to give the source function. The 3D source function was also extracted via direct fits to the 3D correlation function with an empirical Hump function given by

$$S^H(r_x, r_y, r_z) = \lambda \exp[-f_s(\frac{x^2}{4r_{xs}^2} + \frac{y^2}{4r_{ys}^2} + \frac{z^2}{4r_{zs}^2}) - f_l(\frac{x^2}{4r_{xl}^2} + \frac{y^2}{4r_{yl}^2} + \frac{z^2}{4r_{zl}^2})], \tag{6}$$

where $\lambda, r_0, r_{xs}, r_{ys}, r_{zs}, r_{xl}, r_{yl}, r_{zl}$ are fit parameters and $f_s = 1/[1 + (r/r_0)^2]$, $f_l = 1 - f_s$. This procedure corresponds to a simultaneous fit of the ten independent moments. The solid curves in Fig. 2 show the results of such a a fit. They indicate that the 8-parameter Hump function achieves a good fit to the data ($\chi^2/\text{ndf}=1.4$).

3. Source Image and its interpretation

Figures 3(a)-(c) show the source function profiles S(r_x), S(r_y) and S(r_z) obtained via fitting (line) and source imaging (squares). S(r_x) is characterized by a long tail, which is resolved up to $\sim$60 fm; S(r_y) and S(r_z) are resolved up to $\sim$25 fm. The corresponding correlation profiles obtained by summation of the data (circle), fit (line) and image (square) moments are shown in Figs. 3(d)-(f). The broader S(r_x) is associated with the narrower C(q_x) (Fig. 3(a) and (d)), as expected.

The extended tail lies along the pair total transverse momentum. Thus, the relative emission times between pions, as well as the source geometry, will contribute to S(r_x). The source lifetime contributes to the range of S(r_z) and S(r_y) reflects its mean transverse geometric size.

Figure 3: Source function profiles S(r_x), S(r_y) and S(r_z) (left panels) and their associated correlation profiles C(q_x), C(q_y) and C(q_z) (right panels) in the PCMS. The bands indicate statistical and systematic errors.

The difference between S(r_x) and S(r_y) is thus driven by the combination of the emission time difference, freeze-out dynamics and kinematic Lorentz boost.
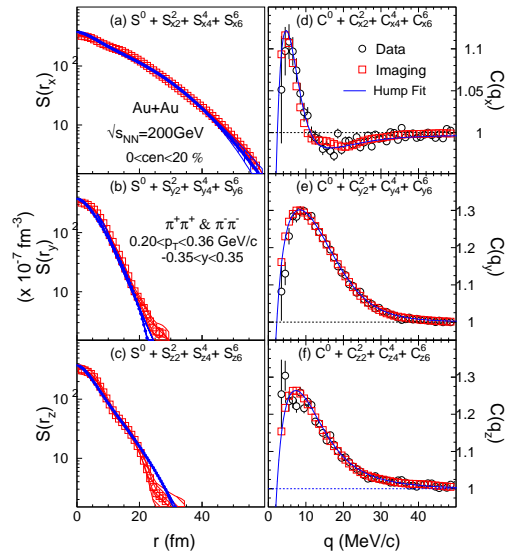
To aid interpretation of the source function, the event generator Therminator [10] was used to predict source functions for several model scenarios. Therminator provides thermal emissions (including all known resonance decays) from a longitudinally oriented, boost invariant cylinder of radius ρ_{max}. A differential fluid element is a ring defined by cylindrical coordinates z and ρ; it breaks up at proper time τ in its rest frame or at time t in the lab frame, where $t^2 = \tau^2 + z^2$. The freeze-out hypersurface is given by $\tau = \tau_0 + a\rho$, where τ_0 is the proper breakup time for $\rho = 0$ and a represents the slope of the freeze-out hypersurface in ρ-τ space; for $a > 0$ particles at small ρ's are emitted at earlier times i.e inside-out "burning"; outside-in "burning" occurs for $a < 0$.

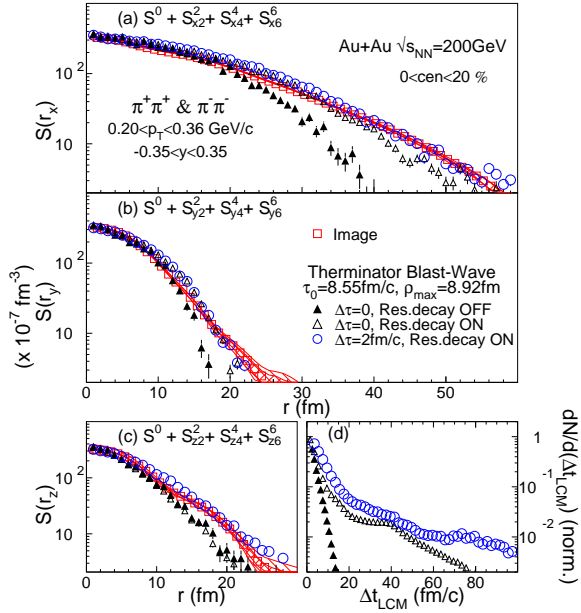Calculations were performed in Blast-Wave mode for a set of parameters tuned

Figure 4: Source function comparison between Therminator calculation and image for (a) $S(r_x)$, (b) $S(r_y)$, (c) $S(r_z)$ in PCMS. Panel (d) compares Δt_{LCM} from Therminator events with various assumptions for $\Delta\tau$ and resonance emission.

to fit charged pion and kaon spectra. In addition, transverse expansion [governed by a radial velocity v_r semi-linear in ρ, i.e. $v_r(\rho) = (\rho/\rho_{max})/(\rho/\rho_{max} + v_t)$ $(v_t = 1.41)$] was assumed and a was varied. The mid-rapidity pion pairs so obtained were also generated with the effects of all known resonance decay processes on and off. The resulting pairs were then transformed to the PCMS, as in the data analysis, to obtain $S(r_{x,y,z})$ distributions for comparison with the data.

Figure 4 shows that the 3D source function generated by Therminator calculations (open triangles) with $\tau_0 = 8.55$ fm/c, $\rho_{max} = 8.92$ fm and $a = -0.5$ with resonances on, reproduce $S(r_y)$ but do not fully account for the long tails in x and z ie. the latter are longer than the Therminator source profiles. For the same parameters, the calculations underestimates $S(r_x)$, $S(r_y)$ and $S(r_z)$ when resonances are turned off (solid triangles). Reasonable attempts to fit the distributions by only increasing τ_0 or with $a \geq 0$ failed, suggesting substantial contribution from pion pairs with significantly longer emission time differences.

An alternative approach to lengthen the distribution of time differences between pion pairs is to sample them from a family of hypersurfaces defined by a range of values of proper breakup times τ'. One such parametrization consists of replacing τ by τ' chosen from an exponential distribution $dN/d\tau' = \frac{\Theta(\tau'-\tau)}{\Delta\tau} \exp[-(\tau'-\tau)/\Delta\tau]$, where the width of the distribution $\Delta\tau$ represents the mean proper emission duration. Figure 4 shows that this approach, with $\Delta\tau = 2$ fm/c (open circles), leads to a fairly good match to the three observed source profiles.

Figure 4(d) summarizes the relative emission time distribution in the LCMS, Δt_{LCM}, for pion pairs from events with the parameterizations indicated. For a fixed $\tau_0 = 8.55$ fm/c ($\Delta\tau = 0$) and resonance decays excluded, the distribution Δt_{LCM} is narrow, $\langle|\Delta t_{LCM}|\rangle = 2.4$ fm/c. The addition of resonance decays adds a long tail and gives $\langle|\Delta t_{LCM}|\rangle = 8.8$ fm/c. Replacing τ with the exponential distribution τ' with $\Delta\tau = 2$ fm/c, results in a Δt_{LCM} distribution which is significantly broadened to give $\langle|\Delta t_{LCM}|\rangle = 11.8$ fm/c. The wider distribution of time delays is needed to reproduce the source distributions. This implies a non-zero proper emission duration in the emission rest frame.

Figure 4 shows that substantial time differences Δt_{LCM} are required to account for the source distensions; however, the interplay between proper time and breakup dynamics is model dependent. Nevertheless, the picture which emerges from the Therminator model comparison is consistent with an expanding fireball ($\rho_{max} = 8.92$ fm) with proper breakup time $\tau_0 \sim 9$ fm/c, which hadronizes and emits particles over a short but non-zero mean proper emission duration $\Delta\tau = 2$ fm/c. Such a short time duration is incompatible with the predictions [2, 3] for a first order phase transition.

4. Conclusions

In conclusion, a novel three-dimensional source imaging technique has been used to extract the 3D pion emission source function in the PCMS frame from Au+Au collisions at $\sqrt{s_{NN}} = 200$ GeV. The source function has a much greater extent in the out (x) and long (z), than in the side (y) direction. Therminator model comparisons suggest an emission source ($\rho_{max} = 8.92$ fm) burning from outside in with proper lifetime $\tau_0 \sim 9$ fm/c and a mean proper emission duration $\Delta\tau \sim 2$ fm/c. These emission characteristics are incompatible with the predictions for a first order phase transition. However, they point to significant relative emission times ($\langle|\Delta t_{LCM}|\rangle \approx 12$ fm/c, including those due to resonance decay) which could result from a crossover phase transition.

5. References

[1] F. Karsch et al., Phys. Lett.B478, 447, 2000.
[2] S. Pratt, Phys. Rev. Lett. 53, 1219, 1984.
[3] Dirk H. Rischke et al., Nucl. Phys. A608, 479, 1996.
[4] M. Lisa et al., Annu. Rev. Nucl. Part. Sci. 55, 357, 2005.
[5] S.S. Adler et al., Phys. Rev. Lett. **98**, 132301 (2007)
[6] P. Danielewicz and S. Pratt, nucl-th/0612076v2 (2007)
[7] P. Chung, J. Phys. G: Nucl. Part. Phys. **35** 044034 (2008)
[8] S. Afanasiev et al., arXiv:0712.4372, (2008)
[9] D. Brown and P. Danielewicz, Phys. Lett. **B 398**, 252 (1997)
[10] A. Kisiel et al, Comput. Phys. Commun. 174, 669 (2006)